GSICS Annual Meeting 2025 March 17 15:30-15:50CST

Long-Term Variations of Cross-Calibration between Himawari-8/SEDA and GOES16/MPS-HI

Tsutomu NAGATSUMA
National Institute of Information and Communications Technology,
Space Environment Laboratory

Space Environment Data Acquisition Monitor onboard Himawari-8,9

SEDA: Space Environment Data Acquisition Monitor

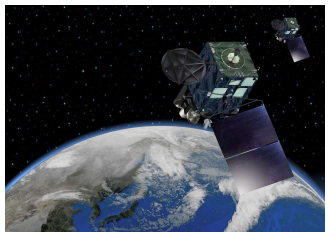

Items	Description
Number of Channels	Protons : 8 (individual 8 sensor elements) Electrons : 8 (8 stacked plates in one elements)
Energy Range	Protons : 20 MeV – 100 MeV Electrons : 0.2 MeV – 5 MeV
Time Resolution	10 sec.
Field of View	Protons : ± 39.35 deg. Electrons : ± 78.3 deg.

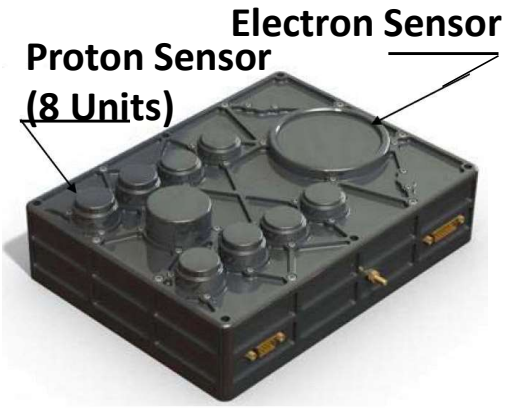

- High-energy particle environment over Japanese sector will be monitored by SEDA as housekeeping purpose.
- Near-real time SEDA data is provided from JMA to NICT. We have been provided SEDA data as part of space weather information.

Himawari-8 Launch: 2014/10/07
Himawari-9 Launch; 2016/11/02
Himawari-8/SEDA data is available from Nov. 03, 2014.

Himawari/SEDA Data Viewer

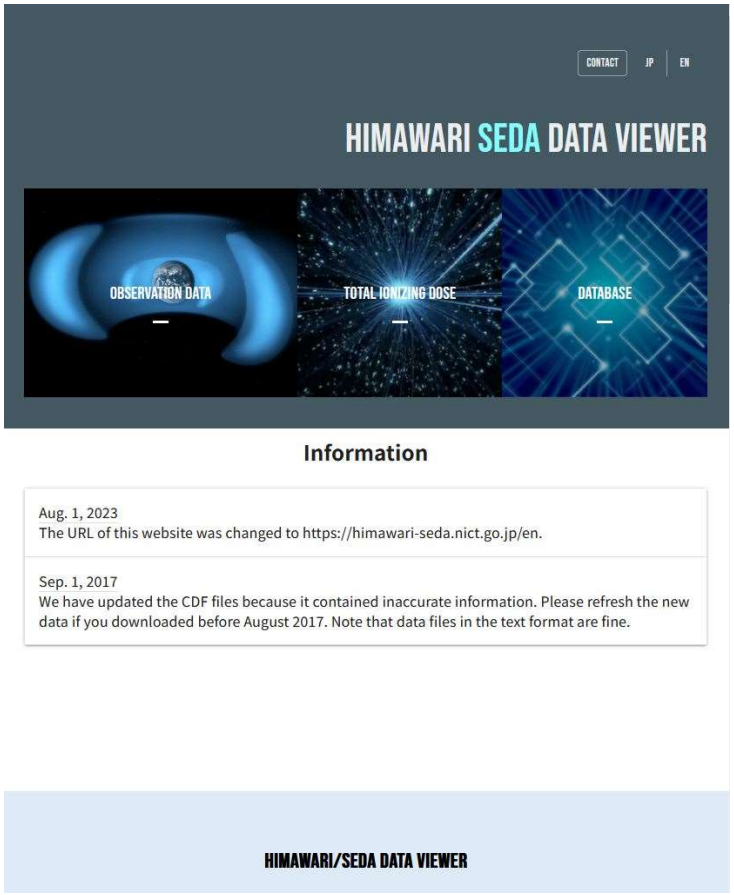

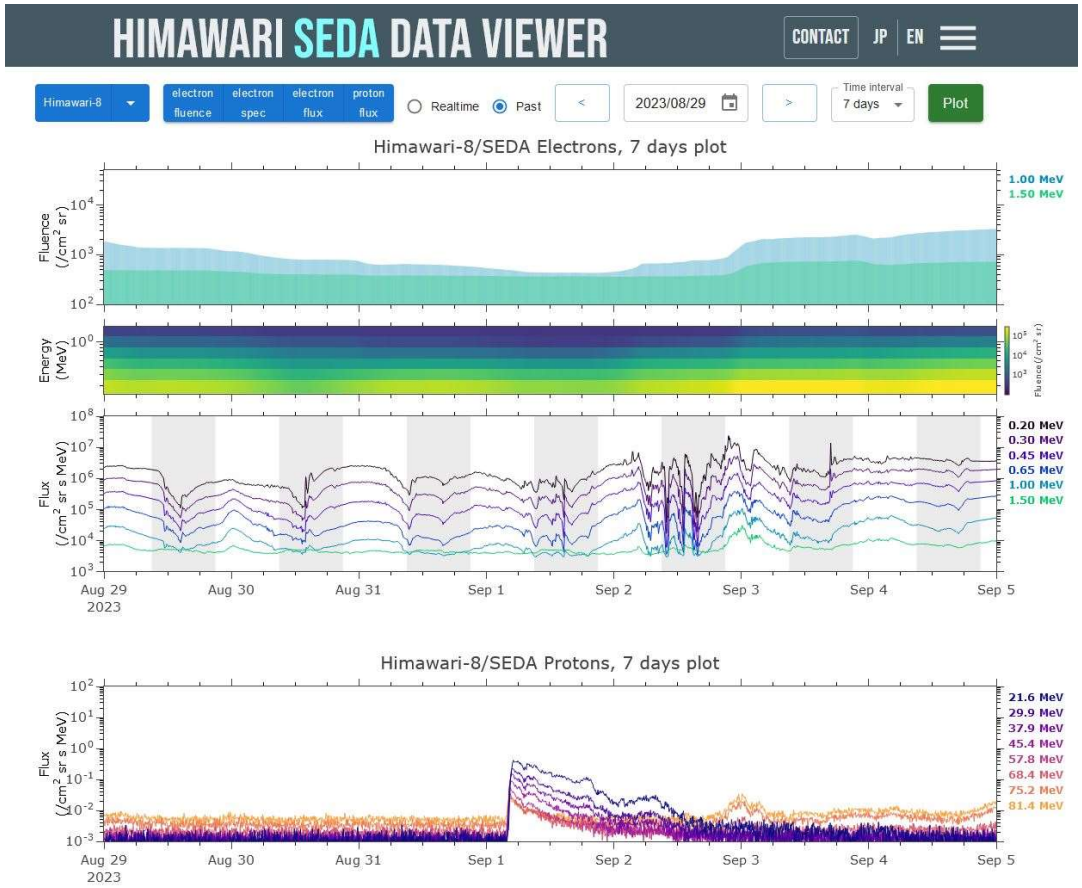

Near-real time SEDA data are able to browse and download from the web site.

https://himawari-seda.nict.go.jp/

SEDA-e: High energy electron measurments

SEDA-e

Ch0: 0.2 MeV
Ch1: 0.3 MeV
Ch2: 0.45 MeV
Ch3: 0.65 MeV
Ch4: 1.0 MeV
Ch5: 1.5 MeV
Ch6: 2.0 MeV
Ch7: 4.5 MeV

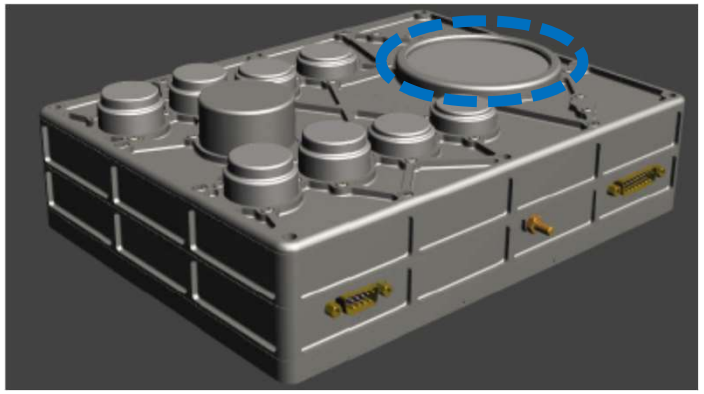

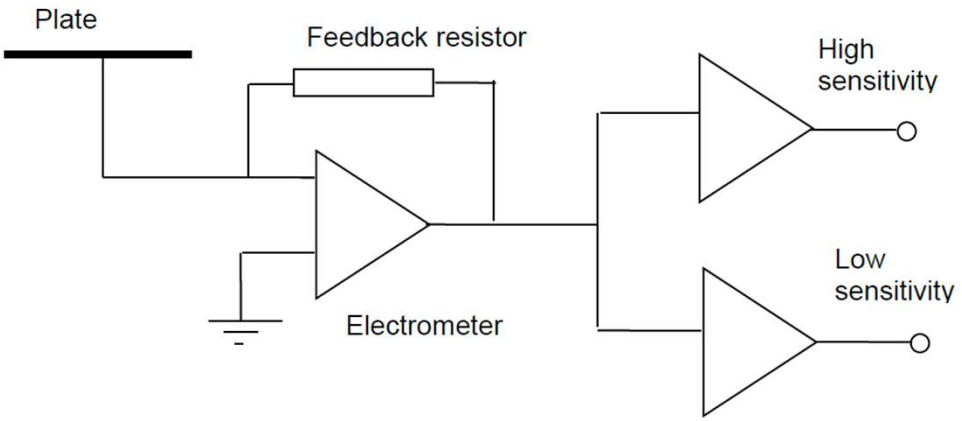

SEDA-e measures internal charging currents produced from high energy electrons (0.1 – 4.5 MeV) collected by 8 plates arranged in a stack. Electron fluxes are estimated from the charging currents. To estimate the charging currents, **bias current (voltage) needs to be subtracted**. Bias current as a function of temperature are estimated based on the ground experiment.

Himawari-8 SEDA-e long term variations (all ch.)

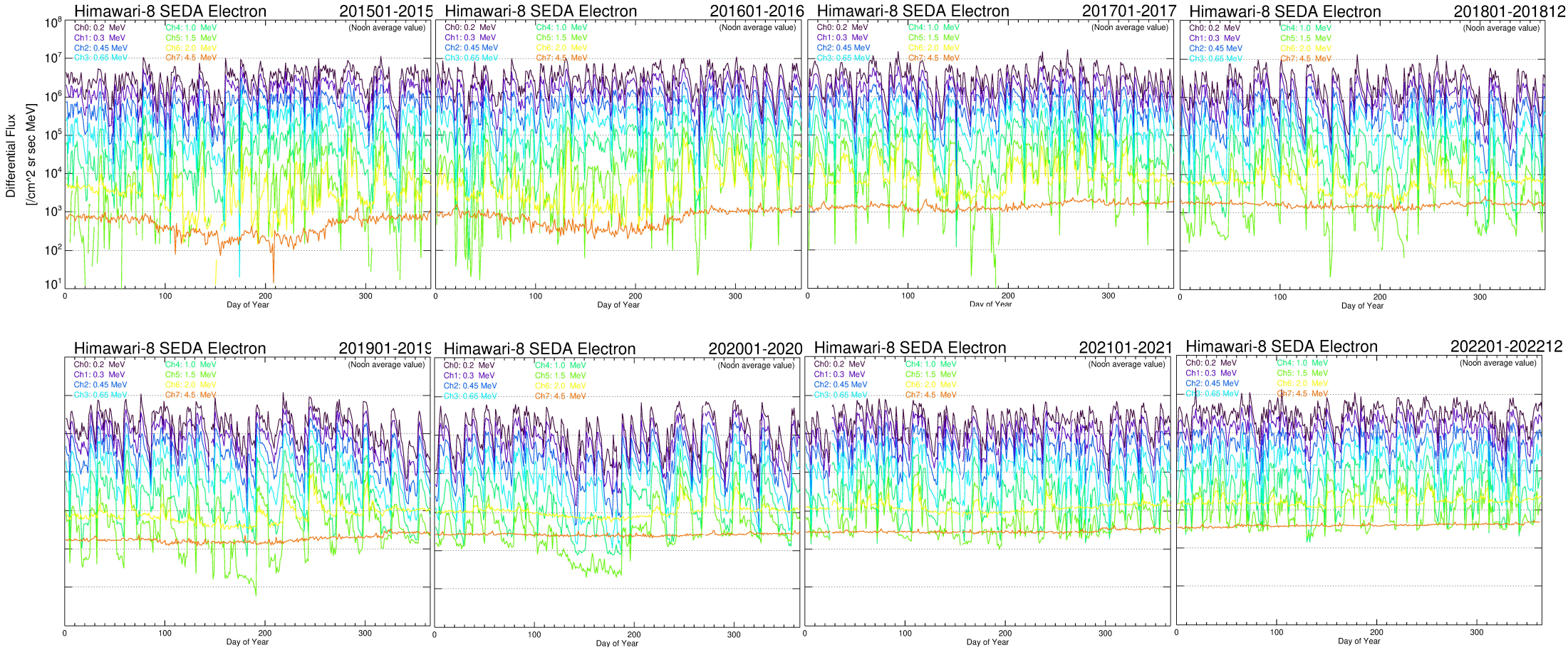

Himawari-8 SEDA-e long-term variations（ch. 6,7）

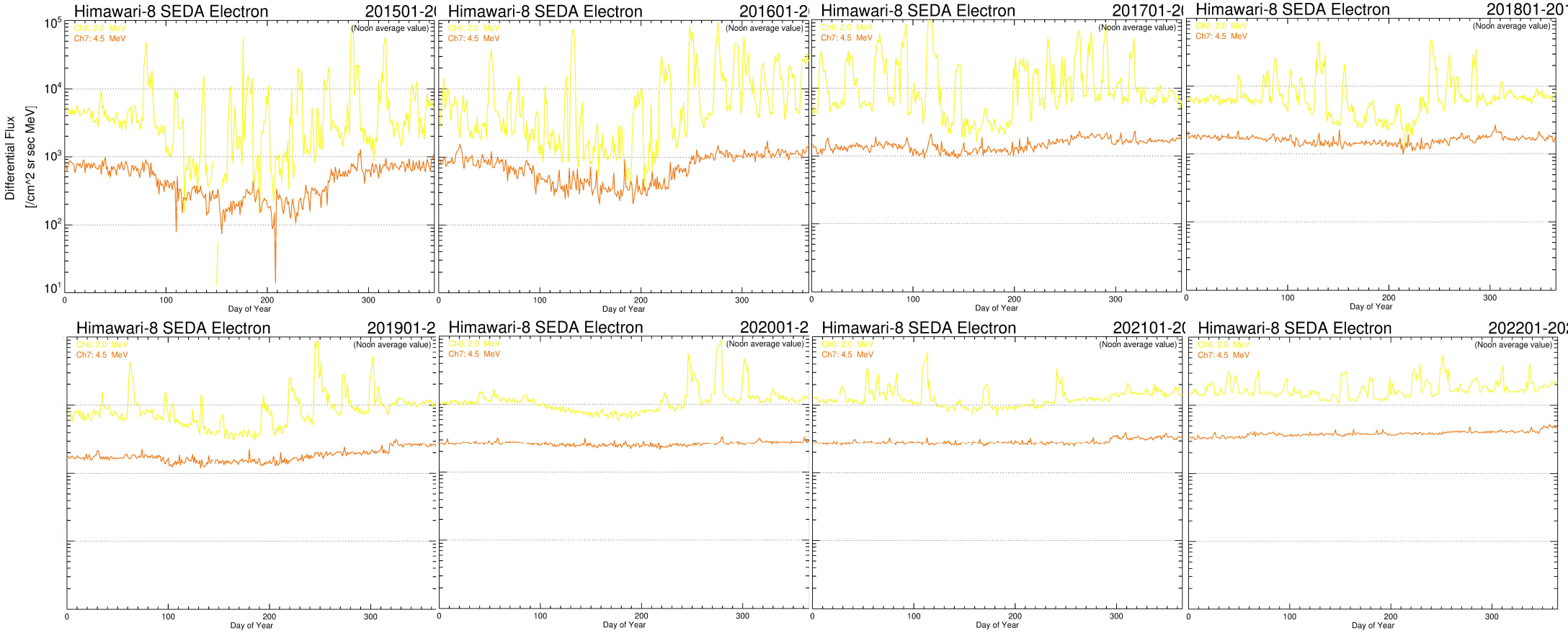

Background noise level of SEDA-e tend to be increased with time goes on.

Seasonal dependence on B. G. flux level of SEDA-e

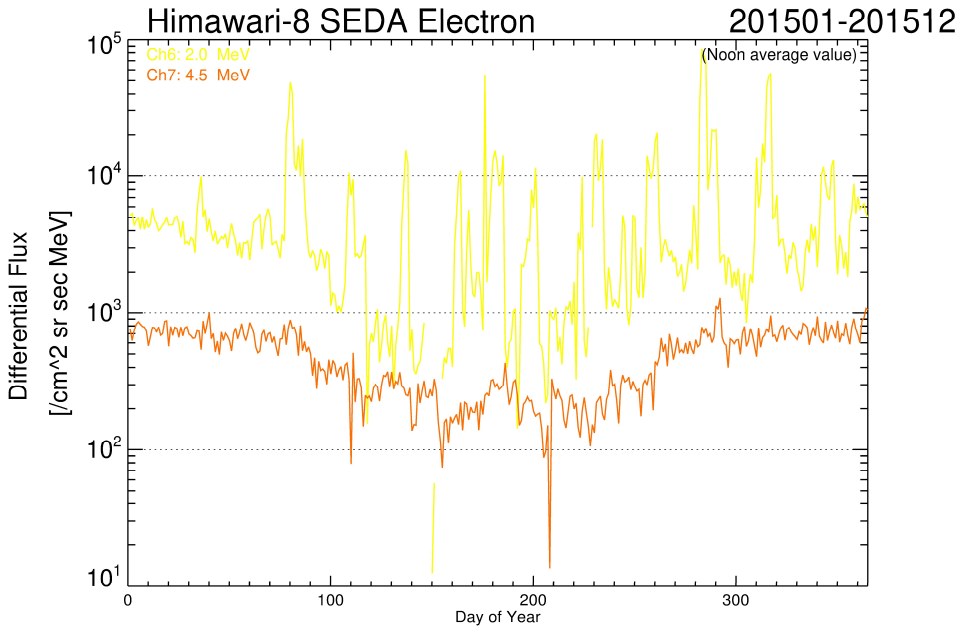

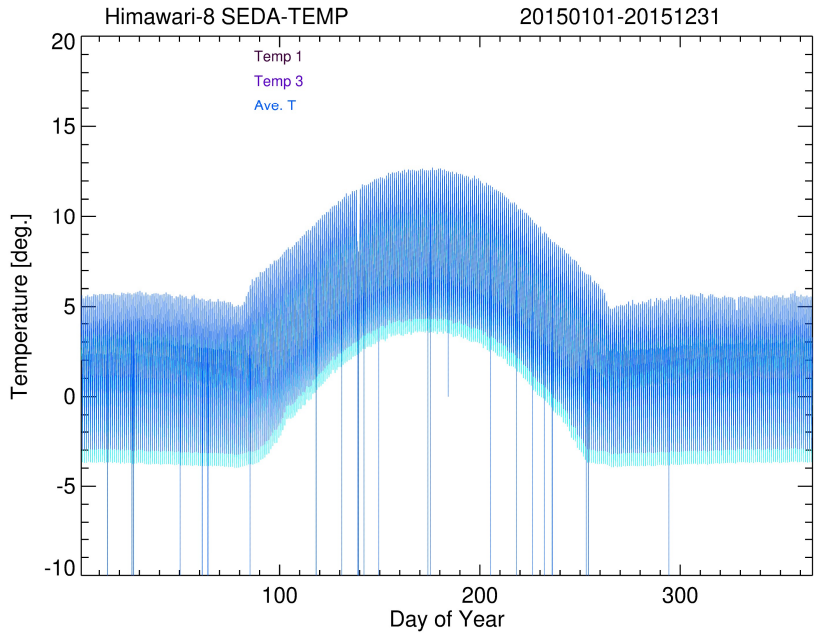

Seasonal dependence of the background flux level corresponds to the temperature variation of the SEDA-e sensor. This might be occurred by the residuals of the bias current subtraction.

The results of improving bias current subtraction

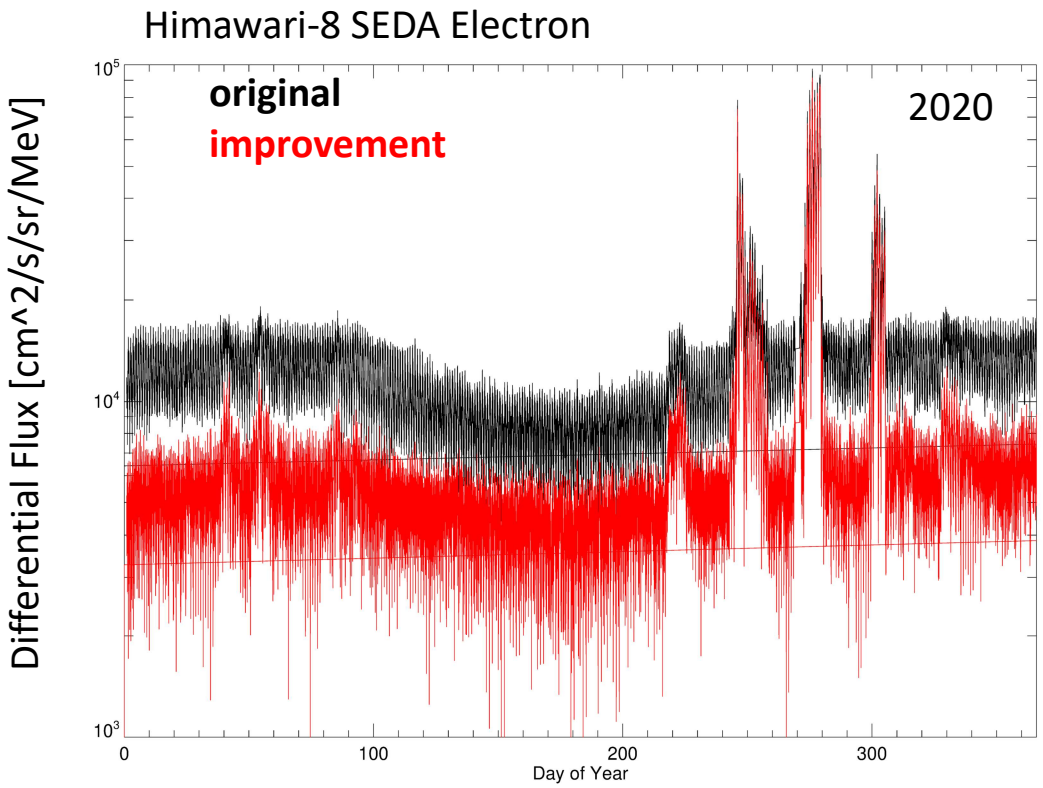

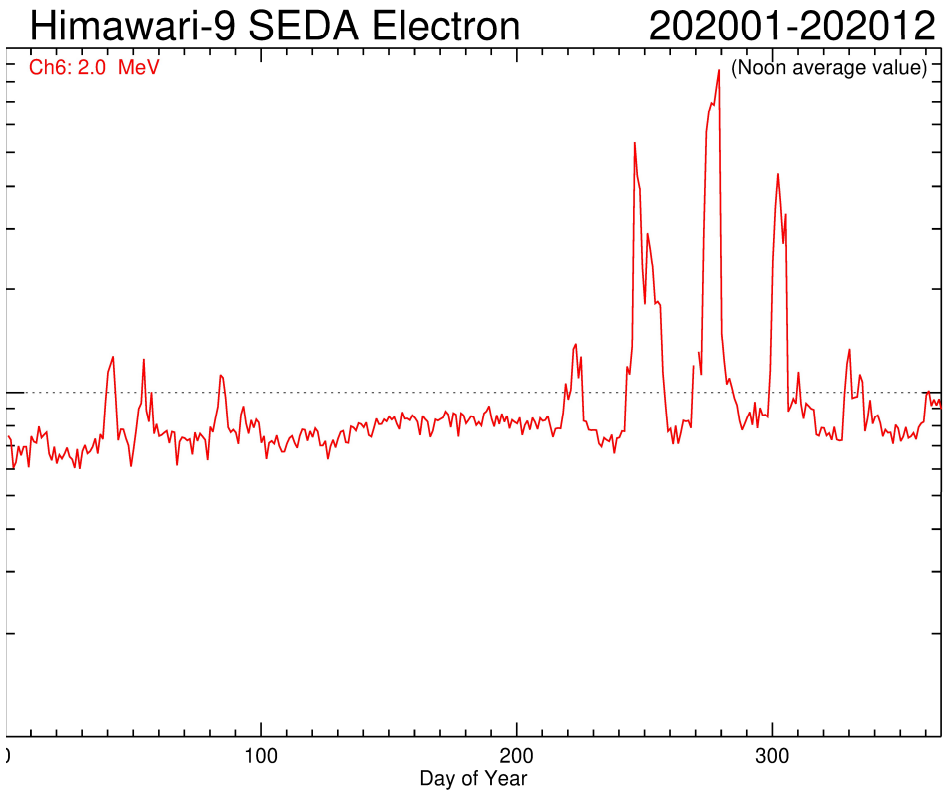

Low flux level tend to be improved due to improvement of bias current subtraction.

Long-term trend of the bias current level

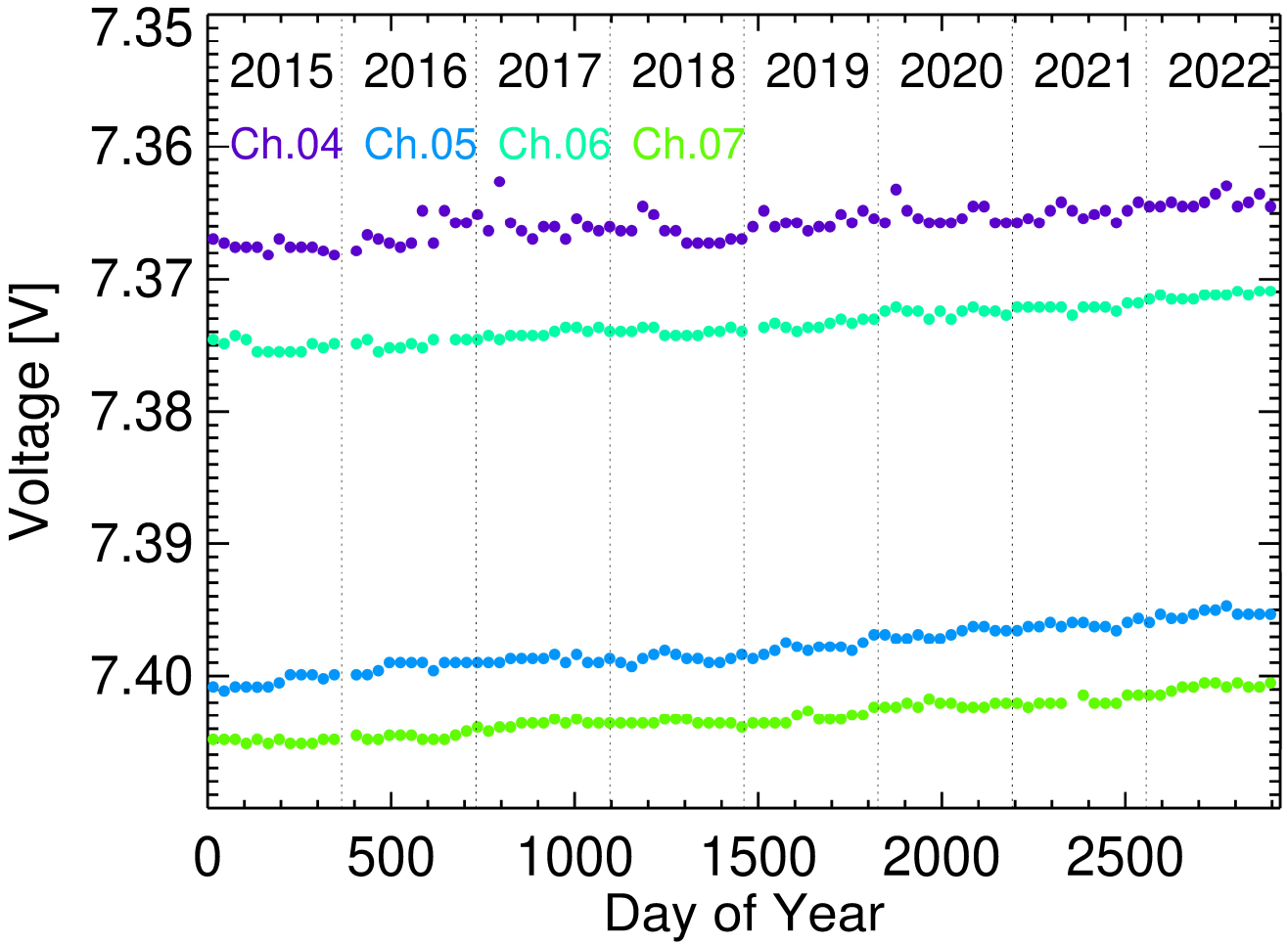

Bias currents tend to be increasing as time goes on.

GOES-16 Space Environment in-situ suite (SEISS) Magnetospheric Particle Sensor – High Energy (MPS-HI)

The MPS-HI sensor monitors medium and high energy protons and electrons.

Electron Energy of each channel [keV]

- E1 : 67.7
- E2 : 131.3
- E3 : 183.1
- E4 : 288.6
- E5 : 412.8
- E6 : 600.3
- E7 : 900.3
- E8 : 1493.1
- E9 : 1969.0
- E10: 2907.2

Interpolation of adjusting SEDA-e channels [keV]

- E0: 200 from MPS-HI E3&E4
- E1: 300 from MPS-HI E4&E5
- E2: 450 from MPS-HI E5&E6
- E3: 650 from MPS-HI E6&E7
- E4: 1000 from MPS-HI E7&E8
- E5: 1500 from MPS-HI E8
- E6: 2000 from MPS-HI E9
- E7: 4500

We use log-linear interpolation

Identify L* conjunction period

- Comparing particle data which observes particles in the same drift shell.
- We should avoid magnetic local time (MLT) around midnight and noon. [Friedel et al., 2005
- L* is calculated using IRBEM library.

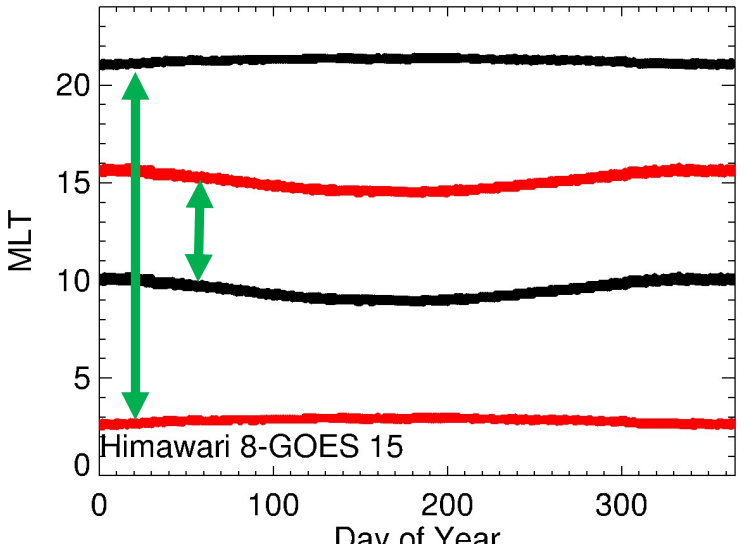

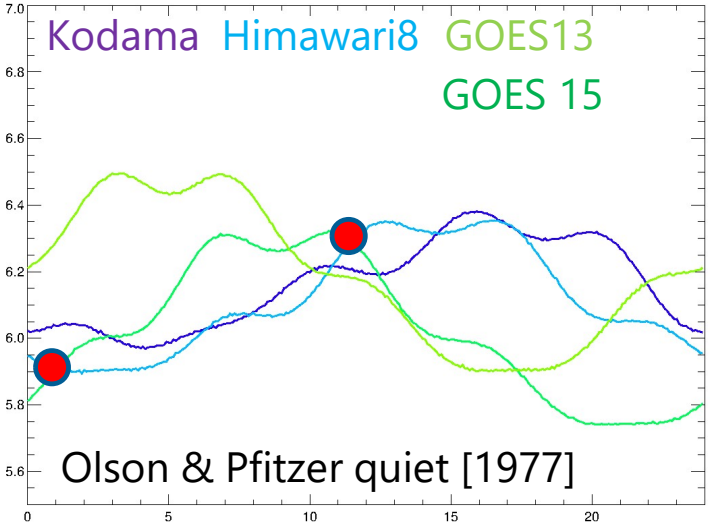

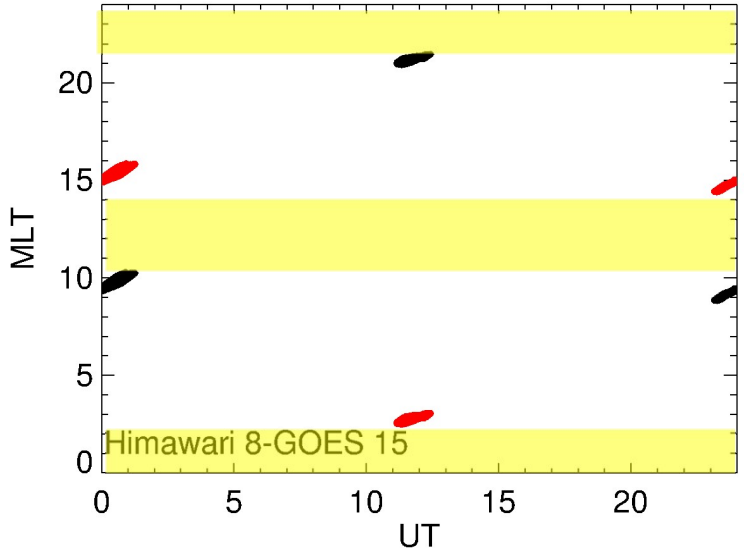

Flux projected to geomagnetic equator

$$f_{eq}(E) = f_{\lambda}(E, \alpha_{\lambda}) \left(\frac{B_{\lambda}}{B_{eq}} \right)^{\frac{m}{2}} / sin^{m} \alpha_{\lambda}$$

$$f_{eq}(E) = f_{\lambda}(E) \left(\frac{B_{\lambda}}{B_{eq}} \right)^{\frac{1}{2}} \qquad \text{If m = 1}$$

- We assume isotropic flux distribution.

Comparison between SEDA-e and MPS-HI

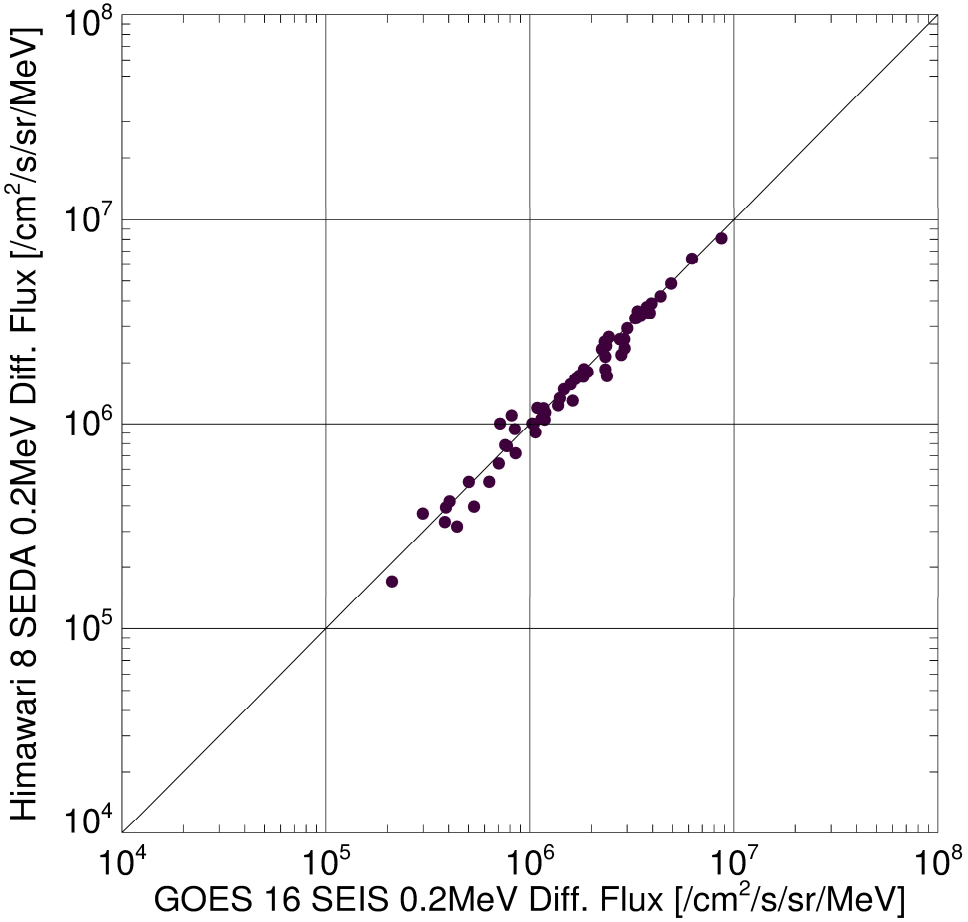

- We use linear fitting to estimate ratio between SEDA-e/MPS-HI.

Long-Term Variation of SEDA-e/MPS-HI(electron)

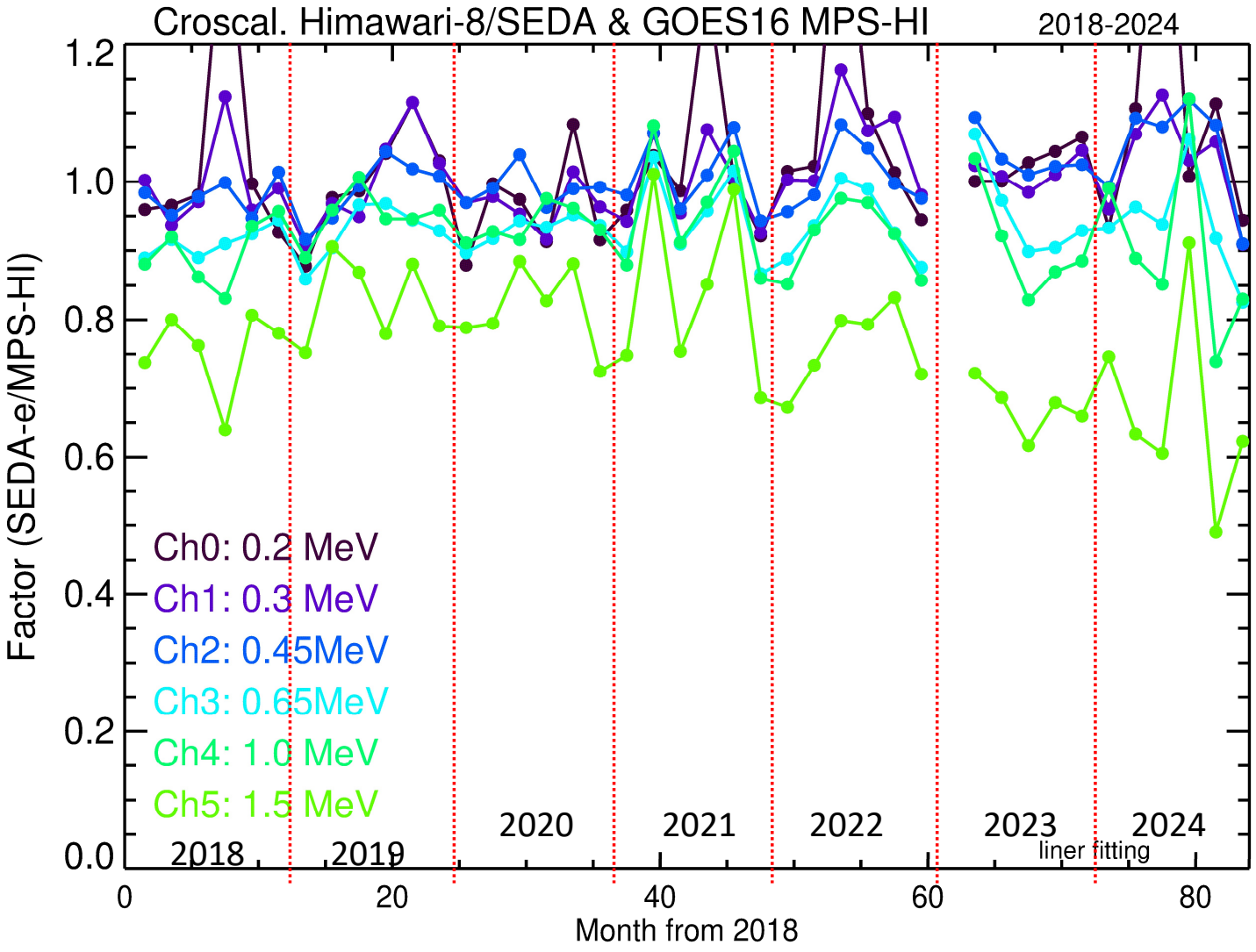

2018/01-02

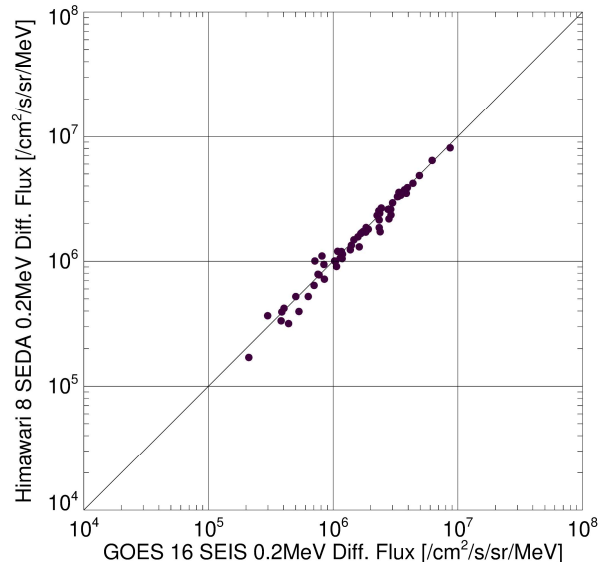
Himawari 8 SEDA 0.2MeV Diff. Flux [/cm²/s/sr/MeV]
GOES 16 SEIS 0.2MeV Diff. Flux [/cm²/s/sr/MeV]

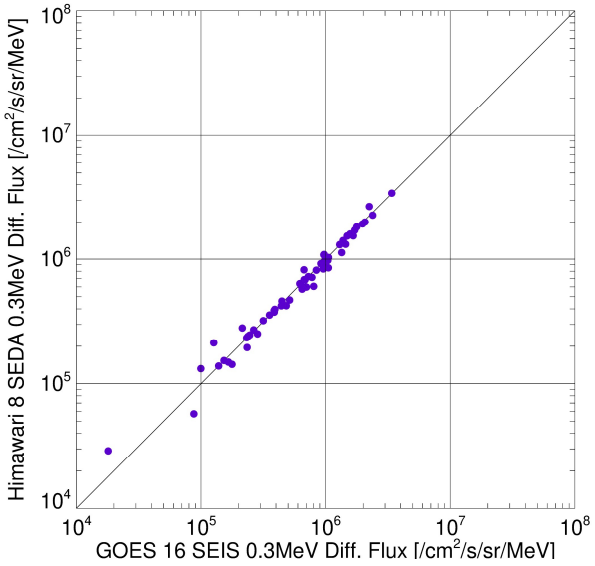
Himawari 8 SEDA 0.3MeV Diff. Flux [/cm²/s/sr/MeV]
GOES 16 SEIS 0.3MeV Diff. Flux [/cm²/s/sr/MeV]

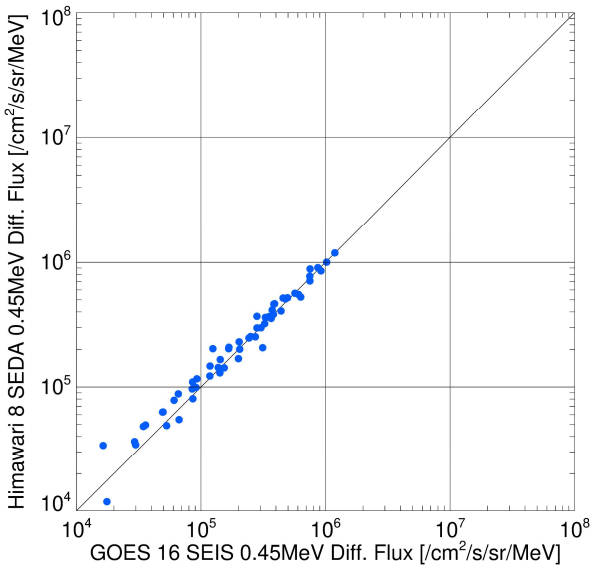
Himawari 8 SEDA 0.45MeV Diff. Flux [/cm²/s/sr/MeV]
GOES 16 SEIS 0.45MeV Diff. Flux [/cm²/s/sr/MeV]

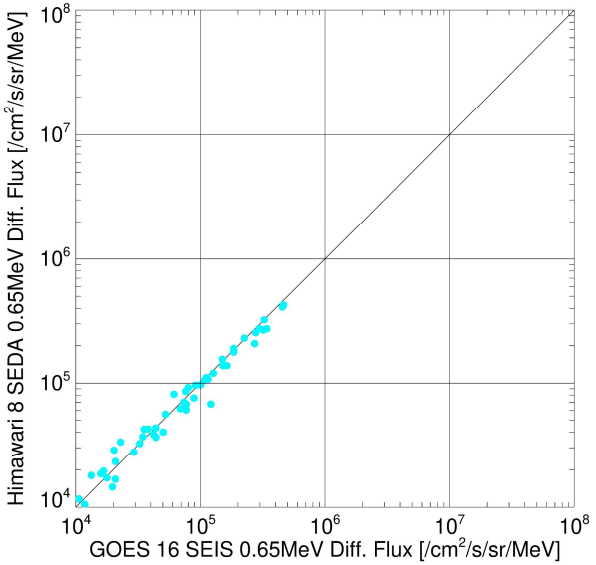
Himawari 8 SEDA 0.65MeV Diff. Flux [/cm²/s/sr/MeV]
GOES 16 SEIS 0.65MeV Diff. Flux [/cm²/s/sr/MeV]

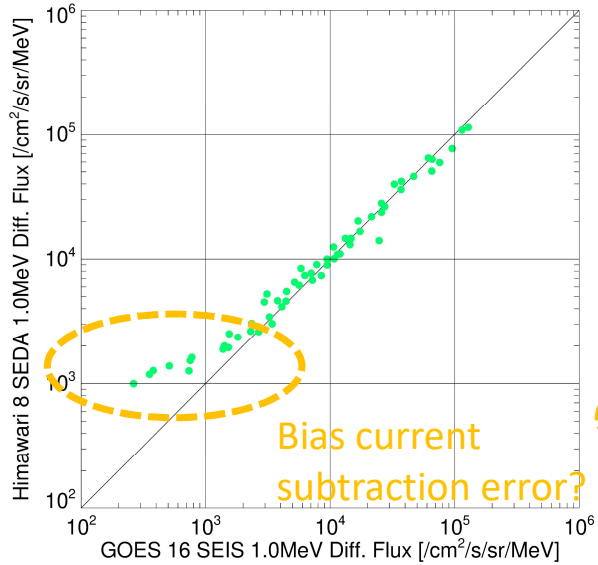
Himawari 8 SEDA 1.0MeV Diff. Flux [/cm²/s/sr/MeV]
GOES 16 SEIS 1.0MeV Diff. Flux [/cm²/s/sr/MeV]
Bias current
subtraction error?

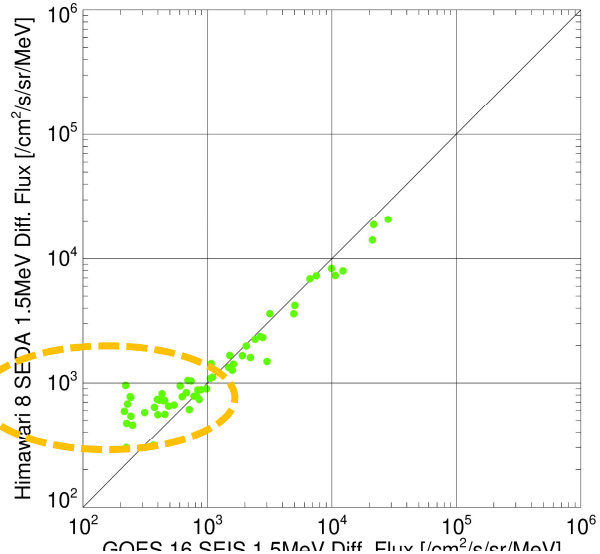
Himawari 8 SEDA 1.5MeV Diff. Flux [/cm²/s/sr/MeV]

2024/11-12

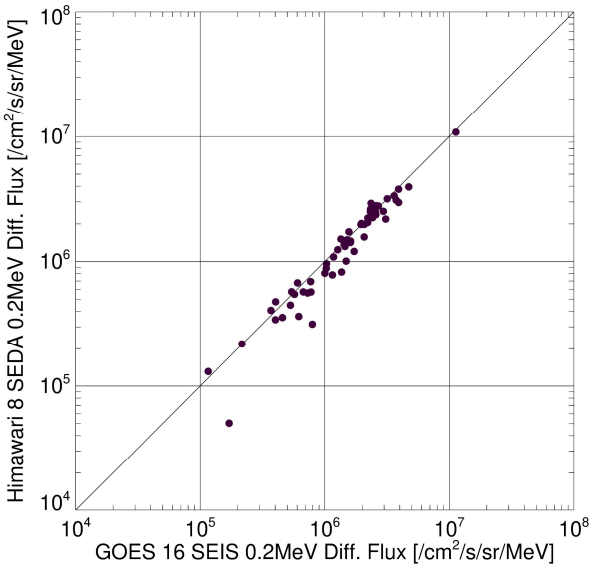
Himawari 8 SEDA 0.2MeV Diff. Flux [/cm²/s/sr/MeV]
GOES 16 SEIS 0.2MeV Diff. Flux [/cm²/s/sr/MeV]

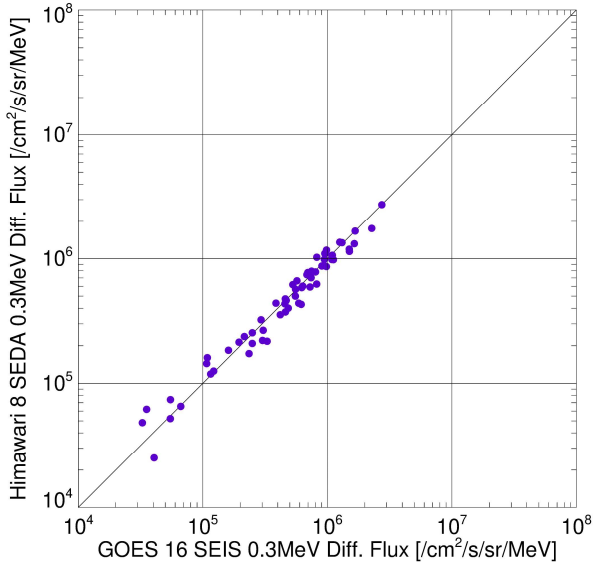
Himawari 8 SEDA 0.3MeV Diff. Flux [/cm²/s/sr/MeV]
GOES 16 SEIS 0.3MeV Diff. Flux [/cm²/s/sr/MeV]

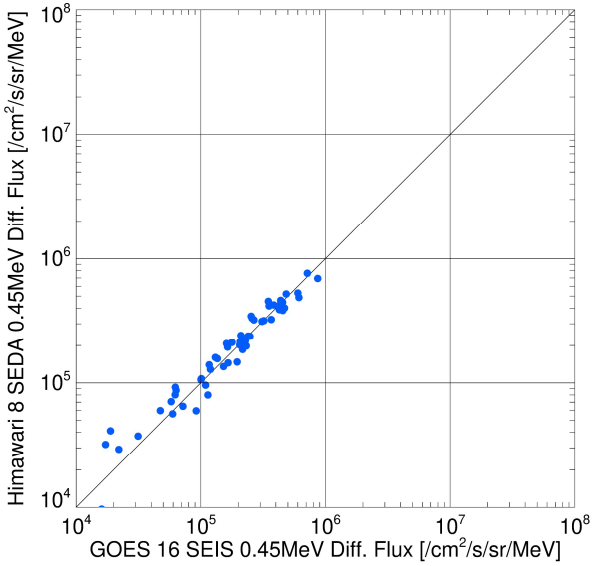
Himawari 8 SEDA 0.45MeV Diff. Flux [/cm²/s/sr/MeV]
GOES 16 SEIS 0.45MeV Diff. Flux [/cm²/s/sr/MeV]

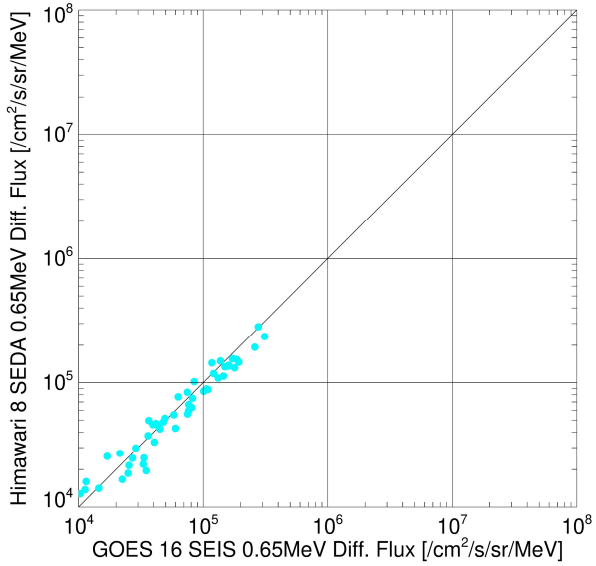
Himawari 8 SEDA 0.65MeV Diff. Flux [/cm²/s/sr/MeV]
GOES 16 SEIS 0.65MeV Diff. Flux [/cm²/s/sr/MeV]

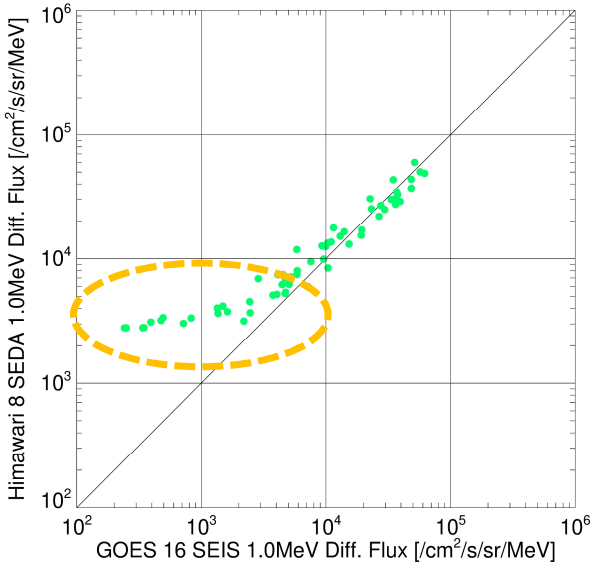
Himawari 8 SEDA 1.0MeV Diff. Flux [/cm²/s/sr/MeV]
GOES 16 SEIS 1.0MeV Diff. Flux [/cm²/s/sr/MeV]

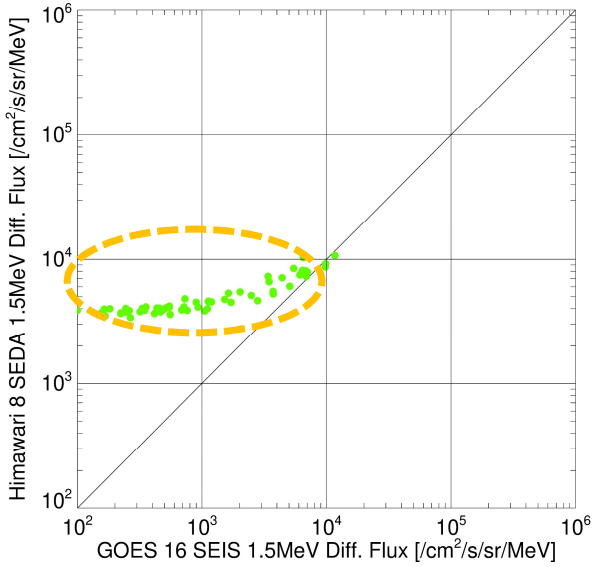
Himawari 8 SEDA 1.5MeV Diff. Flux [/cm²/s/sr/MeV]
GOES 16 SEIS 1.5MeV Diff. Flux [/cm²/s/sr/MeV]

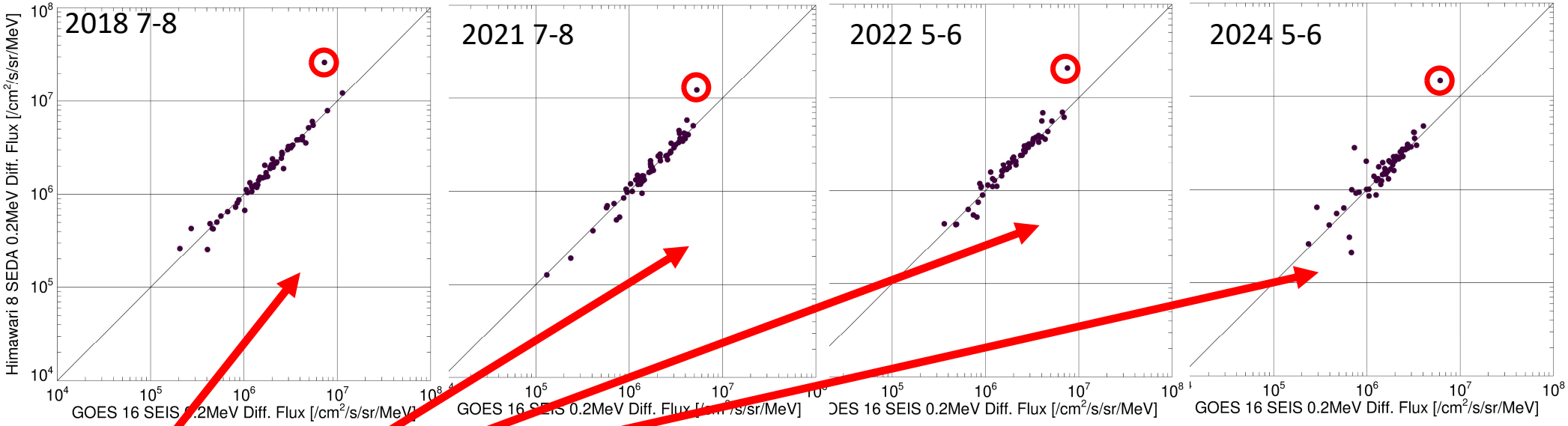

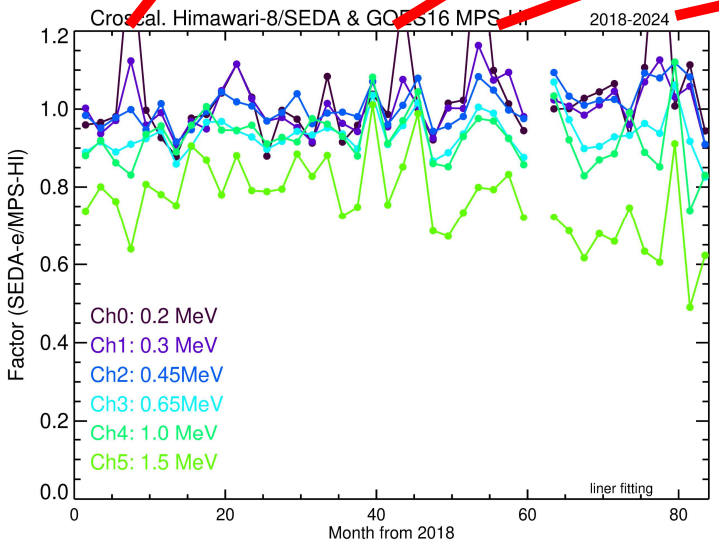

Extreme difference between
SEDA-e and MPS-HI -> Substorm effect?

Summary

- The flux ratios of SEDA-e and MPS-HI are relatively stable up to Ch0-3 of SEDA-e until about 2021, after which the flux ratio change slightly.
- For Ch4-5 of SEDA-e, the influence of bias current is becoming more significant with each year. In the future, it is necessary to establish an algorithm to reduce the influence of bias current on each channel and re-evaluate the results.
- The low-energy channels of SEDA-e may be affected by the short-time flux changes possibly associated with substorms.